Evaluation of Aerodynamic Coefficients of High Temperature Gas Turbine Cascade of Cooled Blade

Dr. Assim H Yousif * & Haider L. Aneed*

Abstract
The aerodynamic force coefficients of five linear cascade of existing film cooling turbine blades are evaluated numerically. The blade is geometrically identical to the first rotor blades of the high pressure (HP) turbine of the F-100-PW-220 military turbofan. Cascade turbine blade test rig has been designed, constructed, and calibrated to introduce experimental work for the same flow conditions of the numerical solution to validate correctness of the numerical results. The numerical simulation shows acceptable agreement with experimental. Also it was found experimentally that both lift and drag coefficients are increased slightly with add of film cooling.

The local Mach number distributions outside the boundary layer on both blade sides of the cascade blade are evaluated numerically and compared with the results of well known CFD code (Fine/Turbo) for existing gas turbine rotor stage of identical blade. The computational results obtained for both cases show that the Mach number distributions trend along both blade sides for rotor stage and cascade are approximately the same, and the values of Mach number of rotor stage are higher than that for the corresponded cascade. Also it was found that the Mach number distributions on both blade sides are reduced in values by the addition of air cooling, and the local Mach numbers for the cascade case is reduced in values among the rotor stage for the two cases with and without film cooling on both blade sides.

Keywords: gas turbine, cascade, stage, Investigation, Mach number, lift coefficient, drag coefficient

تقييم المعاملات الايروديناميكية لصف ريش مبردة لتوربين غازي ذي درجات حرارة عالية

الخلاصة

يتنـاول البحـث الحـالي اجـراء تقيم حسـابي للقـوى الايروديناميـة لصـف مـن خمسـة ريـش توربينيـة خطيـة مبـردة. ان الشـكل الهندسـي للريشـة يماثـل ريـش دوار تـوربين غـازي ذي ضـغط عـالي للمحـرك الحربـي التـورييني النفـاث - F-100-PW-220. ان منصـة الفحـص لصـف ريـش التربـاين تـم تصـميمها وبنائهـا وتـدريجها لاجـراء الجانـب العملـي لـنفس ظـروف الجريـان المسـتخدمة فـي الحـل الحسـابي لاثبـات صـلاحية الحـل الحسـابي. لقـد بينـت المحاكـات الحسـابية توافـق مقبـول مـع الجانـب العملـي. كمـا تبـين ان اضافة هواء التبريد الى النموذج يزيد قيم معاملات الرفع والكبح بشكل طفيف.

كـذالك تـم تقيـيم توزيـع العـدد المـاخي خـارج الطبقـة المتاخمـة علـى جـانبي صـف الـريش وتـم مقارنتهـا مـع النتـائج الحسـابية المستحصـلة مـن البرنـاج المعـروف(Fine/Turbo) CFD code لـريش مماثلـة لمرحلـة دوار محـرك تـورييني غـازي موجـود. ان النتـائج الحسـابية المستحصـلة لحـالتي الـريش بـدون تبريـد وبوجـود التبريـد علـى كـلا جـانبي الـريش بينـت ان سـلوك توزيـع العـدد المـاخي لحـالتي صـف الـريش ومرحلـة الـدوار كانـت متقاربـة بشـكل جيد وان توزيـع الرقم المـاخي لمرحلـة الـدوار كـان اعلـى مـن توزيـع الـرقم المـاخي لصـف الرش. كمـا وجـد ان توزيـع العـدد المـاخي علـى جـانبي الـريش للحـالتين قـد قـل بسـبب وجـود هـواء التبريـد وان الـرقم المـاخي الموضـعي لحالـة صـف الـريش قلـت قيمتـه مقارنـة مـع مرحلـة الـدوار لكلا الحاتين مع وعدم وجود التبريد.

* Machines & Equipments Engineering Department, University of Technology/ Baghdad

Eng. &Tech. Journal Vol. 29 ,No. 8 ,2011

Evaluation of Aerodynamic Coefficients of High
Temperature Gas Turbine Cascade of Cooled Blade

Introduction

The continuous improvement in the performance of air-breathing propulsion systems necessitates a continuous increase in the turbine inlet temperatures. This, coupled with the demands of reduced size of the combustors, has put a significant burden on turbine technology. Since the inlet temperatures of present generation gas turbines are much higher than the melting temperatures of the available alloys used to make the turbine blades, cooling of the blades is a critical issue in turbine technology. In high temperature gas turbines cooling systems need to be designed for turbine blades, vanes, end walls, and other components to meet metal temperature limits. The problem becomes aggravated by the growing trend of using higher turbine inlet temperature to generate more power. Thus, film cooling is used as a cooling mechanism and it works in the form of row of holes in the span wise directions of the blade, from where cold jet is issued into the hot cross flow. The film cooling system is achieved by allowing the working air to form an insulating layer between the hot gas stream and the walls of the blade.

The mixing process during the penetration of the cold jet into the hot gas creates a three-dimensional complex flow field. A recent study of three dimensional thermal effect of the turbine blade film cooling and the penetration area of jets issuing at an angle into cross mainstream flow is reported numerically and experimentally by [1]. The film cooling on concave and convex surfaces create a three-dimensional complex flow field. The film cooling effectiveness and heat transfer coefficient on concave and convex surfaces with one row of injection holes inclined stream-wise at 35° was investigated by [2]. Also the aerodynamics effect of coolant flow blowing, the mixing losses and the

wake flow generated downstream of two dimensional turbine blade cascades were
also investigated experimentally by [3] and studied numerically by [4].

The gas turbine combustion chambers and turbine blades require better cooling techniques to cope with the increase in operating temperatures with each new engine model. Transpiration-cooled components have proved an effective way to achieve high temperature and erosion resistance for gas turbines operating in aggressive environments as reported by [5], in which in this study the current gas turbine inlet temperatures approaching 2000 °K.

Effusion cooling is a relatively simple and more reliable than the transpiration-cooled components. The effusive cooling system of gas turbine was studied recently by [6]. The studies represent a numerical model suitable to design the geometric features of effusive cooling systems of gas turbine, and to evaluate their thermo-fluid-dynamic characteristics.

From the above selected survey, which has so far been discussed, it is clear that the literature survey voluminous. But there is lack of information about the effect a wide variety of flow condition, as a matter of fact the presence of film cooling, specially the aerodynamic forces coefficients generates on the blade. At

the present work numerical modeling approach will be performed to estimate the blade aerodynamics coefficient and flow field characteristics and the effect of film coolant injection will be taken into account. Numerical simulation under turbulent conditions of flow through stationary cascade blades passage is performed to simulate three-dimensional complex flow field of mixing process of the cold jet and the hot gases. A first stage rotor blade of cooling blade cavities and film cooling orifices will be used to produce the cascade blades passage as given by [7]. Experimental investigation of identical cascade of five linear blades is also introduced to validate the accuracy of the numerical code. The same values of $(T_{in}, T_{jet}, P_{in} and P_{out})$ given by [7] are used in the present work to predict the cascade blade Mach number distribution. The numerical results of well known Fine/turbo codes are also used to validate the numerical approach.

Experimental set-up and procedure

Experimental work was performed on open jet type low speed wind tunnel designed and manufactured to use at the present investigation. A five blades gas turbine cascade, consist of two end walls between which the constant section blades (rotor blade of first stage of high pressure gas turbine of F-100-PW-220 engine) are placed in the wind tunnel open jet. Two adjusting blades in the cascade are used to simulate the blades passage with blowing cooling system. The (210) circular holes are used to simulate the coolant jet holes in the pressure side of blade, while (90) holes were used to simulate the coolant jet holes on the suction side of the blade, the lateral distance between each two

neighboring holes is 3D. Figure (1) shows photos of the jet hole rows location on both blade sides and internal coolant passage cavitations. Table (1) also indicated the jet hole rows location as a percentage distance from the chord

The present experimental rig includes the following parts:

a- Open jet low speed wind tunnel as shown in figure (2).

b- The mass flow rate is controlled by changing the test rig inlet area by using manual gate throttling valve and by changing the fan and the fan rotational speed. The suitable rotational speed is achieved by variable frequency AC controller (0.4-22 KW), (200v/400v) type (LS variable frequency), which able to vary the rotational speed between zero and 3000 rpm. The cascade assembly is shown in figure (3).

c- Test section consists of five blades distributed at equal pitch distances to form a linear turbine blade cascade.

d- Coolant injection system, compressed air system, discharged the air through small holes (forward-lateral expanded hole on the blade outer walls).

e- Pressure regulating valve to control the pressure of injected air from the compressed air tank.

Each row of holes has different jet inclination angle similar to the actual blade jet angle of the real turbine. The jet angles of each row are also tabulated in table (2), the dimensionless for the blade cascade $(d/c) = 14.8 \%$.

The Cascade

The aerofoil span was fixed as 20 cm to assure that the flow near the central region of the cascade, where the flow measurements are made, is approximately two-dimensional. The

geometric parameters of the cascade are listed in table (3). The wall surfaces on both blades sides were coated by varnish in order to make the blades surfaces as smooth as possible. Figure (3) show the cascade blade assembly. A standard Ogival Pitot-static tube is used to measure cascade upstream air flow velocity at the middle of the test section. Correction was made to the Pitot static tube reading according to British standard.

A devise conical tip head five-hole pressure probe, the probe has the shape of a truncated cone, was used to measure the downstream flow, velocity vector, and stagnation pressure. The devise is a stream lined symmetric body that points into the flow. The pressure distribution on the surface of the probe depends on the angle of incidence of the main flow vector relative to the axis of the probe. Central pressure tap gives the conventional stagnation pressure when the flow vector is perpendicular to the point on the surface. Nil reading of pitch angle pressure taps is related to the flow direction. (i.e. flow deflection inclination angle (α_2)).

The Reynolds number (Re) based upon the blade cord and the mainstream velocity during the experimental program was $2.3*105$.

Referring to Figure (4), in which represent one passage of cascade blade according to [2]. The flow assumed to be incompressible and the flow formula is used because the change of density is negligible. With using cascade notation for velocities and angles as given in [8],

$$\Delta p = \frac{1}{2}(v_1^2 - v_2^2) - \overline{w}$$

or

$$= \frac{1}{2}\rho v_a^2(tan^2\alpha_1 - tan^2\alpha_2) - \overline{w} \qquad \dots (1)$$

The axial velocity v_a being assumed the same at inlet and out let. The axial force per unit length of each blade is $s\Delta p$ and from consideration of momentum changes, the force acting along the cascade per unit length is given by

$$F = s\rho v_a \times change\ in\ velocity\ component\ along\ cascade$$

$$F = s\rho v_a^2 \times (tan^2\alpha_1 - tan^2\alpha_2) \qquad \dots (2)$$

The coefficients C_L and C_D are based on a vector mean velocity v_m defined by the velocity triangles. Thus

$$v_m = v_a\ sec\ \alpha_m$$

Where α_m is given by

$$tan\ \alpha_m = \frac{1}{2}(tan\ \alpha_1 + tan\ \alpha_2)$$

The drag and lift coefficients according to [8] are given by the following equations

$$C_D = \left(\frac{s}{c}\right)\left(\frac{\overline{w}}{\frac{1}{2}\rho v_1^2}\right)\left(\frac{cos^3\alpha_m}{cos^2\alpha_1}\right) \qquad \dots (3)$$

And

$$C_L = 2\left(\frac{s}{c}\right)(tan\ \alpha_1 - tan\ \alpha_2)cos\ \alpha_m - C_D\ tan\ \alpha_m \qquad \dots (4)$$

Numerical Investigation

FLUENT Software Package has been used in present numerical investigation. Preprocessor step is the creation of geometry by using the AUTOCAD-2009. The circular jet holes creation is done by the path (Operation → Geometry → volume → create real cylinder) and then rotate and move the hole by the dimension and angle given in the table (2), and then aligning the geometry by the path (Operation → Geometry → volume → unite real volumes) and then rotate the geometry by 45° angle using the path way command (Operation → Geometry → Face → move → rotate), as shown in Figure (5).

Eng. &Tech. Journal Vol. 29 ,No. 8 ,2011

Evaluation of Aerodynamic Coefficients of High
Temperature Gas Turbine Cascade of Cooled Blade

The program structure creates the grid by using GAMBIT software. T- Grid is used to generate a tetrahedron and hexahedron, which are existing boundary mesh. The computational grid in this case contains 72426 grid modes. The mesh generation is shown in Figure (6).

At this step boundary conditions must be specified. The computational domain, see Figure (7), is choosing identical to the experimental domain in order to make a fair comparison between experimental and computational result.

At Inlet boundary, the inlet pressure is specified. It's suitable for incompressible flow calculations and it can be used when the inlet pressure is known. Outlet boundary conditions required specified static pressure. The value of the specified static pressure is only used while the flow is subsonic [9]. The wall boundary conditions are used to bind the fluid and solid regions. The entire velocity component is set to zero on all solid boundaries (blade surfaces) except at the lateral walls (end walls) the shear stress is set to zero. Periodic boundary conditions are used when the physical geometry of interest and the expected pattern of the flow solution have a periodically repeating nature. There are two types of periodic boundary conditions:

1. Translational periodic boundary.
2. Rotational periodic boundary.

The translational periodic boundary conditions are used when the pressure drops across translational periodic boundaries. The Rotational periodic boundary conditions are used when no pressure drops across periodic planes. The Translational periodic boundary and the Rotational periodic boundary are types of symmetry boundary condition. When applying this boundary condition, it is required to set the flux of all variables leaving the outlet periodic boundary equal to the flux entering the inlet periodic boundary on the opposite side [11]. This is achieved by equating the values of each variable at the nodes just upstream and downstream of the

inlet plane to the nodal values just upstream and downstream of the outlet plane. The injection total air temperature and pressure are taken constants along the blade span and equal to the cooling air temperature. The static pressure assumed to be the same at holes exist for cold jet and main stream flows The blowing ratio between air jet velocity and main flow stream velocity was taken constant for all jut holes and equals to (2) as recommended by [4].

Processor step is the solution by solving NAVIER-STOKES equations (continuity and momentum equations), and energy equation, as well as, the turbulence flow model. The computational results were examined with using five turbulence models available in the computational cod used to find the correctness of the CFD code prediction. These models are (standard (k-ε), RNG (k-ε), realizable (k-ε), standard (k-ω) and SST (k-ω)). Each turbulence model was individually reviewed. Postprocessor step was done by reviewing the results of the computational code.

The computational code gave C_L and C_D values by using different turbulence models. The RNG (k-ε) model performed close values to the experimental of C_L and C_D than the standard (k-ε) model. The results were tabulated in table (5) for both cases with and without film cooling. Reference [11] found that RNG (k-ε) models performed correct pressure distributions than the other turbulence model, when he predicted the pressure distributions on both turbine cascade blade surfaces, in The RNG (k-ε) model is the modified form derived from standard (k-ε) model by using statistical technique called Renormalization Group theory. It has an additional term in the transport equation for (ε), which improved the accuracy of the model for highly strained and swirling flows. Also an analytically derived formula for

effective viscosity has also been added to the RNG (k-ε) model, which account for the low (Re) effects on the near wall region. This required a suitable treatment near wall region. According to [12], this model reduces the rate production of (k) and dissipation (ε) [13]. Also RNG (k-ε) model represent the strain dependent term in the transport equation for (ε) [13].

Mach number distributions

The turbine enter and exit conditions obtained from flight data [7] of F-16 fighter aircraft are used as the input data for the gas turbine simulation program (GSP). This program is a tool for gas turbine performance analysis, developed at National Aerospace Laboratory of the Netherlands (NLR), and enables to simulate both steady state and transient condition for any kind of gas turbine configuration. The simulation is based on one dimensional modeling of the processes in the various gas turbine components with thermodynamic relation and steady state characteristics 1].

For the high pressure gas turbine engine investigated at the engine design point the engine data obtained from (GSP) program are given in table (6). The design point corresponds to military thrust, static thrust with after burner at sea level for ISA conditions. Mach numbers and velocities u in the jets from the cooling holes are taken as given by [7].

The contours of Mach number along the axial direction on the cascade blade of identical first stage rotor blade with and without film cooling at the engine reference point are presented in Figures (8) and (9). From these two Figures (8 and 9) one can concluded that the predicted Mach distributions, especially near the leading edge are

considerably difference in values for the two cases, with and without film cooling.

Figure (10) shows that the Mach number distribution outside the boundary layer on a cascade blade at the engine reference point derived from Mach number contours presented in Figure (8). The Mach number distribution outside the boundary layer on the first stage rotor blades without film cooling at the engine reference point as obtained by [7] is also presented in Figure (10), in which they obtained results from aerodynamic calculations of the flow conditions in the high pressure turbine performed with the FINE/Turbo code (Numerical (FINE/Turbo) CFD code available at NLR) [14]. This CFD model solves the Reynolds-averaged Navier-Stokes equations, complemented with a classical algebraic turbulence model (Baldwin-Lomax).

Figure (11) shows the same results presented in Figure (10), but with the presence of film cooling. In both predicted cases the mass presented in Figures (8 and 9) flow rate and flow stagnation pressure and temperature at the turbine entry as well as the static pressure at the turbine exit are the same.

For all cases indicated in Figures (10) and (11), the Mach number on suction side is greater than unity at $(x/c \approx 0.75)$ for both rotor stage and the cascade. The Mach number is reduced in all cases by the addition of cooling air up to the suction peak at $(x/c = 0.75)$.

The local Mach numbers are lower for the cascade case among the rotor stage one for the two cases with and without film cooling on both blade sides. Especially near the leading edge considerable differences are predicted.

As reported by [7] the mass added by the film cooling reduces the local flow Mach numbers in

To understand this reduction in the Mach number an experimental investigation comparing the rotor results with rectilinear cascade of identical geometry done by [15] may be explained these predicted Mach numbers differences. For rotor loss includes the rotor to stator interaction He found the turbine rotor loss higher than that of the cascade by approximately 50 %. Also he found that the loss increase largely independent of spacing between rotor and stator. In modern turbomachine, as for present engine, the spacing between the blade rows is typically of the order of (1/4 to 1/2) of a blade chord. Also the flow in real machine, however, is unsteady both as a result of the relative motion of the blade wakes between the blade rows and potential flow influence. The effects of potential influence extend upstream and downstream and decay exponentially with a length scale typically of the order of blade chord or pitch [8]. As attempts are made to make turbomachines more compact, the level of unsteadiness is increased, therefore the turbine rotor loss increases more.

As seen from the above discussion that the turbine rotor loss is higher than that of the cascade. As a matter of fact the increase of losses reduces the inlet stagnation pressure to the rotor. Also at subsonic speed the reduction in the inlet stagnation pressure will leads to reduce the local Mach number. These remarkable conclusions explain the difference in values between rotor and cascade. Also the Mach number distributions calculated by [7] were made on the complete turbine with respect to aerodynamics and on the

first stage rotor blade. Also FINE/Turbo is used by [7] to calculate the heat transfer coefficient without film cooling and these coefficients are used for both cases. In that case the local Mach numbers are slightly different compared to the situation with film cooling.

Conclusions

The present numerical simulation shows an acceptable agreement with experimental results for the same flow conditions. The numerical simulation of cascade blade with using RNG (k-ε) and k-ω (SST) turbulence models with using film cooling gave the best C_L and C_D values when compared with experimental but not absolutely for all cases. The difference between the local Mach number distribution obtained by FLUENT code for the cascade blade and FIN/TURBO code for the rotor stage for the two cases with and without film cooling on both blade sides. The Mach number is reduced in all cases by the addition of cooling air up to the suction peak at ($x/c = 0.75$). CFD methods require very fine computational grids to realistically capture the flow and near the film cooling injection orifices, this leads to computation times that are out-of-balance.

List of symbols

C_D Drag coefficient
C_L Lift coefficient
c   chord, m
D   Drag, N
D_d Duct diameter, m
d   Diameter of jet hole, m
F   Force, N
k   Turbulent kinetic energy, m^2/sec^2
M   Mach number
P_{in} Inlet pressure, N/m^2

P_{out} Outlet pressure, N/m^2

Re   Reynolds number

T_{in} Inlet temperature, °K

T_{Jet} Temperature of jet film cooling, °K

s   Cascade blade pitch, m

v_1 Inlet flow velocity, m/sec

v_2 Outlet flow velocity, m/sec

v_a Axial velocity, m/sec

v_m Mean velocity, m/sec

w   Velocity in z-direction, m/sec

$\overline{W}$ Stagnation pressure difference, n/m^2

x, y, and z Cartesian coordinate axis,

θ_{Jet} Angle of inclination of jet injection, degree

α_1, α_2, and   Inlet, and outlet flow angles respectively, degree

α_m Mean deflection angle, degree

ε Dissipation rate of turbulent kinetic energy, m^2/sec^3

ρ Air density, kg/m^3

ω Specific dissipation rate, 1/sec

ΔP Pressure difference, N/m^2

References

[1] Yousif, A. H, Al-Khishali, K. J, and Kassim, M. S, " Three Dimensional Investigation of Leading Edge Film Cooling Jets in a Cross Flow", Al Mustanseria University journal, 2011.

[2] Min-Sheng Hung , "Effects of injection angle orientation on concave and convex surfaces film cooling", Department of Biomechatronic Engineering, National Chiayi University, Chiayi 600, Taiwan 2009.

[3] Yousif, A. H, and Shareef, A. S., "Mixing Losses Investigation Downstream of Turbine Blade Cascade with coolant flow blowing". Journal of Engineering Science & Technology, JESTEC, Volume 6, Issue 3, 2011.

[4] Yousif, A. H, and Shareef, A. S., "The effect of blowing ration upon wake flow of turbine cascade blade", Third Scientific Conference, University of Wassit, 9-10/12/ 2009.

[5] Giovanni Cerri, "Advance in effusive cooling techniques of gas turbines", Science Direct, Applied Thermal Engineering, 27, pp 692-698, 2007.

[6] Yousif, A. H, "Thermal Effect of Effusive Cooling Injected through Squire Holes: Detailed Numerical Simulations and Flow Visualizations", the 7th Jordanian International Mechanical Engineering Conference (JIMEC'7), 27 - 29 September 2010, Amman – Jordan

[7] De Wolf, W.B., Woldendorp, S. and Tinga, T., "Analysis of combined convective and film cooling on an existing turbine blade" National Aerospace Laboratory NLR-TP-148, paper No 35, 2001.

[8] Cohen, H., Rogers, G., and Saravanamuttoo, H.,"Gas turbine theory" pp. 322, 2006.

[9] Fluent. 6., Users Guide, (2001)

[10] Versteeg H.K., and Malalasekera W., "An Introduction to Computational Fluid Dynamics the Finite Volume Method", Book, Longman Group, London, 1996.

[11] HAKEM. T. K., "Effects of turbulence modeling on RANS simulation of turbine blade cascade flow field" M.Sc of

Eng. &Tech. Journal Vol. 29 ,No. 8 ,2011

Evaluation of Aerodynamic Coefficients of High
Temperature Gas Turbine Cascade of Cooled Blade

Machines and Equipments, University of Technology, 2010.

[12] Easom, G., J., "Improved turbulence models for computational wind engineering" Ph.D thesis in civil engineering, university of Nottingham, 2002.

[13] Yalchot, V., and Orszag, S., A., "Renormalized group analysis of turbulence" I-Basic theory, J. of scientific computing Vol. 1, No.1, pp. 3-51, 1986.

[14] Numeca International, FINE/Turbo User Manual (version 4.1), Numeca International, Brussels, April 2000.

[15] Hodson, H., P., "boundary layer and loss measurements on the rotor of an axial flow turbine" J. Eng. For gas turbine and power trains Am. Soc. IVG, 391-9, Mech-engrs., 198

Eng. &Tech. Journal Vol. 29 ,No. 8 ,2011

Evaluation of Aerodynamic Coefficients of High
Temperature Gas Turbine Cascade of Cooled Blade

Table (1) Jet holes location as a percentage distance of the chord

Row	$\left(\dfrac{x}{c}\right)$ %	$\left(\dfrac{y}{c}\right)$ %	$\left(\dfrac{D_d}{c}\right)$ %
Row 1	5.55	7.4	8.89
Row 2	17.55	19.62	8.89
Row 3	37.04	25.92	8.89
Row 4	57.4	15.18	8.89
Row 5	74	14.81	4.44

Table (2) location of the jet holes and its inclination angle

hole	$\left(\dfrac{x}{c}\right)$ %	$\left(\dfrac{y}{c}\right)$ %	θ_{jet} [°]
a	14.17	30	90
b	2.48	15.54	100
c	-1.01	1.03	220
d	1.7	-0.68	245
e	5.33	0.074	260
f	10.36	3.3	320
g	22.5	11.65	300
h	37.43	16.16	285
i	55.7	15.2	260
j	74.6	9.88	300

Table (3) Cascade Geometry

Number of blades		5
Chord	[cm]	13.5
Axial chord	[cm]	12.5
Blade stagger angle	[°]	25
Pitch	[cm]	12.5
Span	[cm]	20
Inlet flow angle	[°]	20
Blade inlet angle	[°]	18
Solidity		0.925

Table (4) experimental lift and drag coefficients of (with and without film cooling).

Re	Without film cooling			With film cooling		
	C_L	C_D	$\dfrac{C_L}{C_D}$	C_L	C_D	$\dfrac{C_L}{C_D}$
2.3×10^5	3.953	1.9227	2.056	3.805	2.044	1.8615

**Table (5) Predicted lift and drag coefficients for both cases
(with and without jet injection)**

Turbulence model	Re	Without jet injection			With jet injection		
		C_L	C_D	$\dfrac{C_L}{C_D}$	C_L	C_D	$\dfrac{C_L}{C_D}$
(k-ε) (standard)	2.3×10^5	3.7703	2.1005	1.7949	3.7685	2.1118	1.7845
(k-ε) (RNG)	2.3×10^5	3.7962	2.0747	1.7951	3.7892	2.07152	1.7914
(k-ε)(realizable)	2.3×10^5	3.7704	2.0918	1.8024	3.7672	2.0984	1.7952
(k-ω) (standard)	2.3×10^5	3.7729	2.0812	1.8128	3.7631	2.0805	1.8087
(k-ω) (SST)	2.3×10^5	3.7933	2.0981	1.8079	3.7894	2.0992	1.8051

Table (6) Gas turbine Simulation Program (GSP) results

	HP turbine entry	HP turbine exit	
Total pressure	21.369	5.5643	bar
Static pressure	21.15	5.414	bar
Temperature	1509	993	K
Shaft speed	12910		rpm

Eng. &Tech. Journal Vol. 29 ,No. 8 ,2011

Evaluation of Aerodynamic Coefficients of High
Temperature Gas Turbine Cascade of Cooled Blade

(a) Blade suction side jet hole rows

(b) Blade pressure side jet hole rows

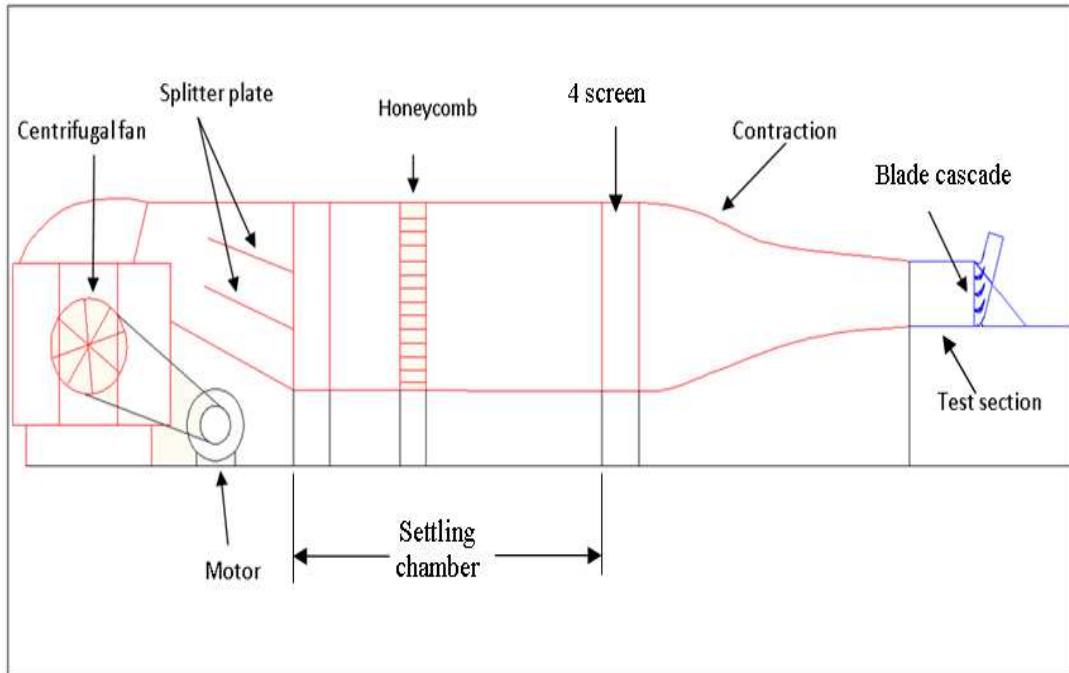**Figure (1) Blade jet holes rows on both suction and pressure sides**

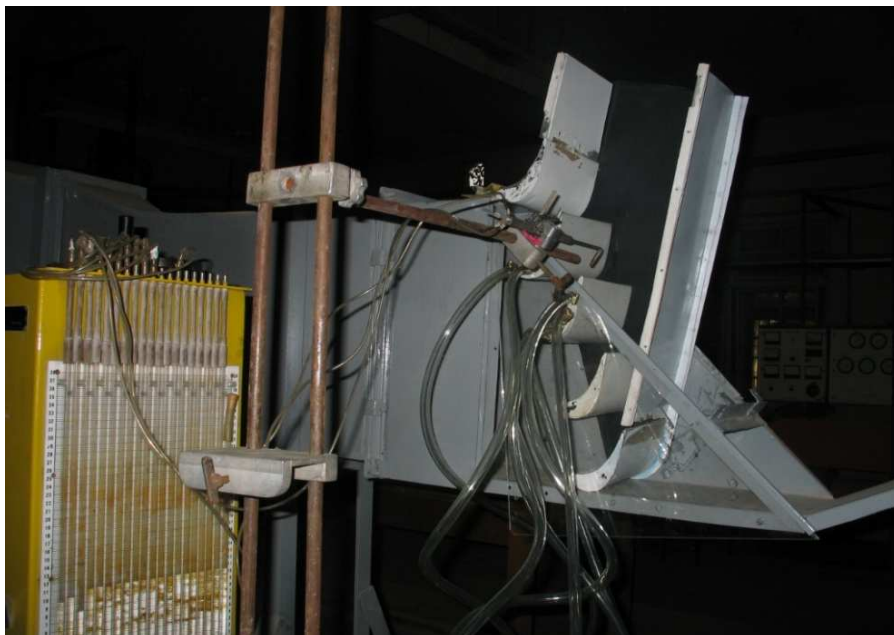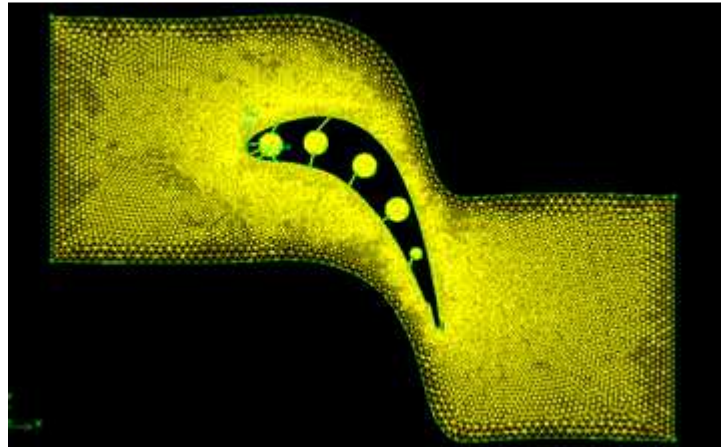**Figure (2) Open jet type low speed wind tunnel**

Figure (3) Cascade assembly

Figure (4) applied and effective forces acting on cascade [8]

Figure (5) Circular holes drawing

Figure (6) Mesh Generation
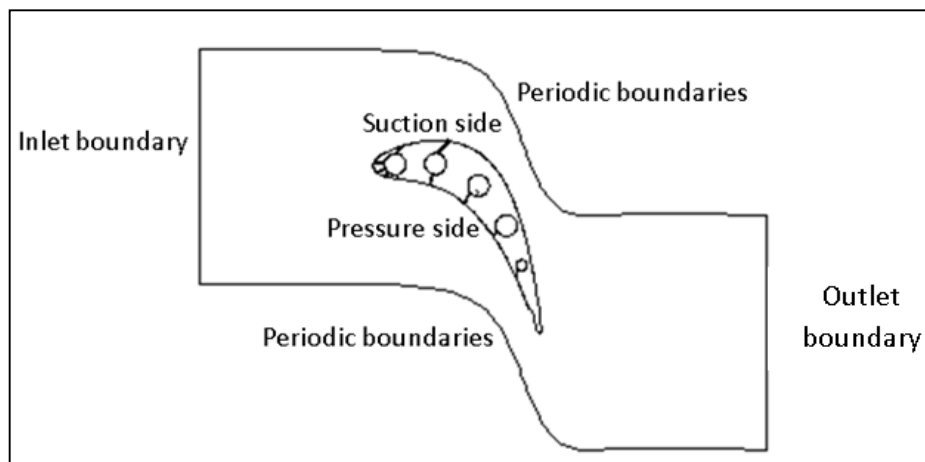
Figure (7) Computational domain
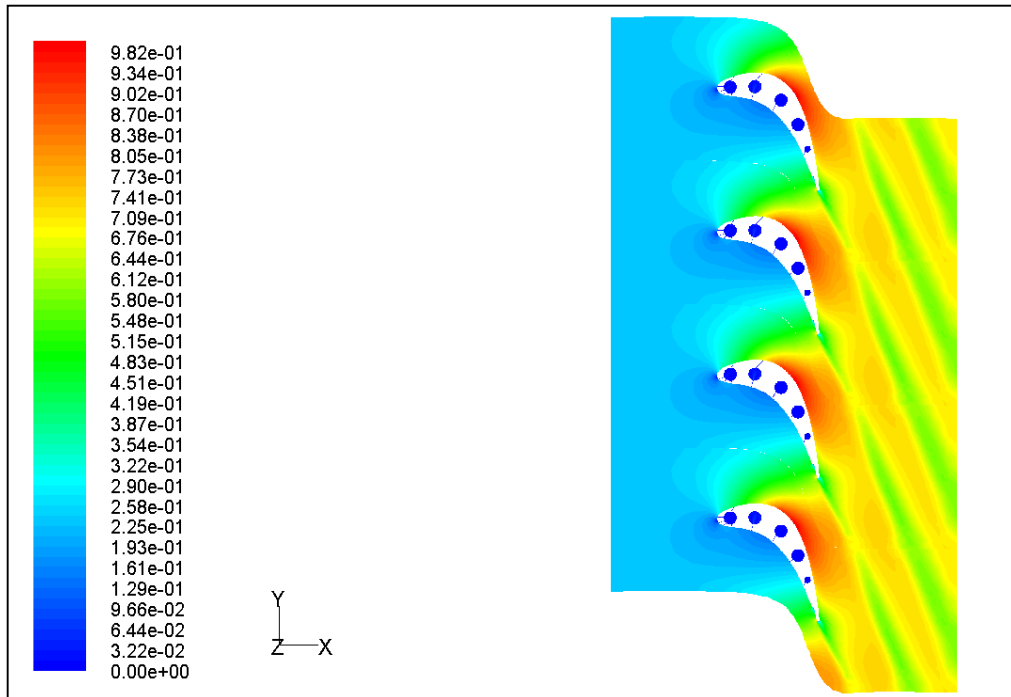
**Figure (8) Mach number contours in cascade blade without film cooling at
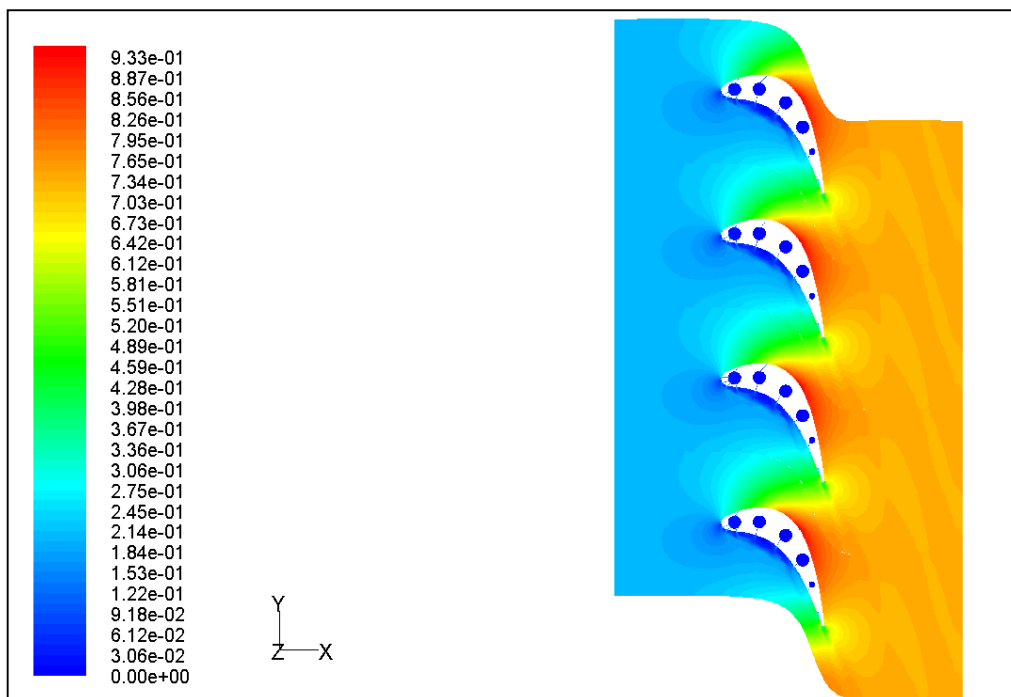engine reference conditions**

**Figure (9) Mach number contours in cascade blade with film cooling at engine
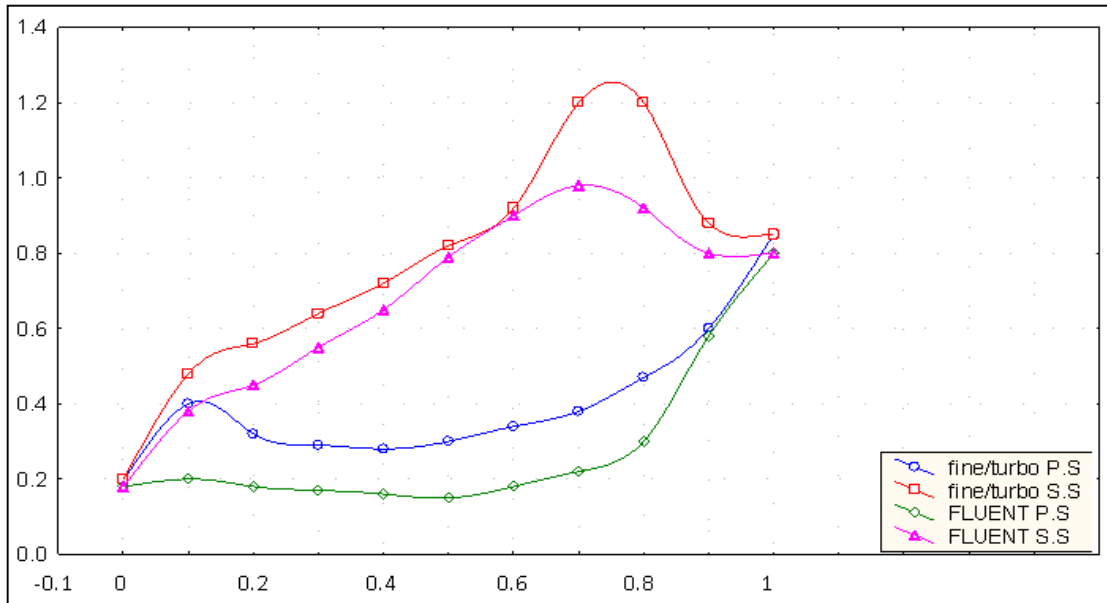reference conditions**

Figure (10) Predicted Mach number distribution on bothe blade side for cacade and rotor stage using FLUENT and FINE/TURBO codes recipectively, with out film cooling
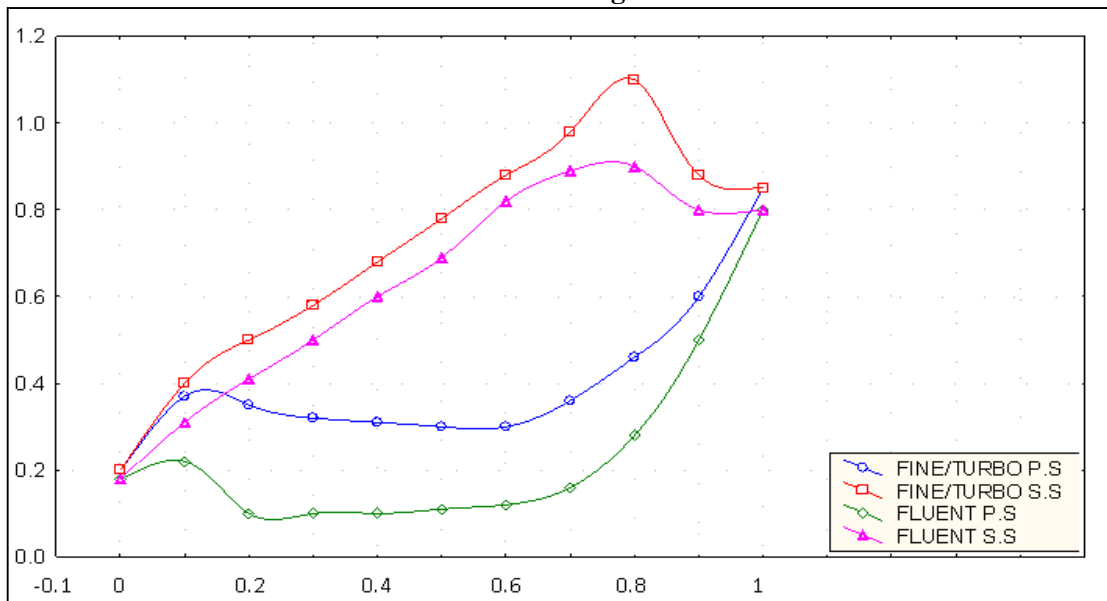

Figure (11) Predicted Mach number distribution on bothe blade side for cacade and rotor stage using FLUENT and FINE/TURBO codes recipectively, with film cooling